Received: 18 June 2026 | Revised:03 August 2026 | Accepted: 18 August 2026

https://doi.org/10.56946/jce.v5i2.957
Volume 5 (2): 1-16

Journal of Chemistry and Environment

Research Article

Tailoring Hydrophobicity: Synthesis, Characterization and Application of Pyridinium-based Surfactants as Corrosion Inhibitors

Maham Almas[1*], Rabia Talat[1,2*], Ubaid Ullah Khan[3*], Saira Fatima[1], Ali Haider[1,4*], Syed Mustansar Abbas[5], Saqib Ali[1]

[1]Department of Chemistry, Quaid-i-Azam University, Islamabad 45320, Pakistan.
[2]Department of Chemistry, Rawalpindi Women University, Satellite Town, 6th Road, Rawalpindi, Pakistan.
[3]Department of Chemical Sciences, University of Lakki Marwat, KPK, Pakistan.
[4]Pakistan Academy of Sciences, 3 Constitution Ave, G-5/2 Islamabad, Pakistan.
[5]Nanoscience and Technology Department, National Center for Physics, Quaid-i-Azam University Campus, Islamabad, Pakistan.

*Corresponding Author: Ali Haider (ahaider@qau.edu.pk); Ubaid Ullah Khan (ubaidullahkha0307@gmail.com); Maham Almas (malmas@chem.qau.edu.pk); Rabia Talat (rabiatalat@chem.qua.edu.pk)

Abstract

This was due to the effect of the alkyl chain length on the critical micelle concentration (CMC), adsorption behavior, and corrosion inhibition of CR4 mild steel in an acidified chloride solution (3.5 wt.% NaCl, pH 1.5) of a series of pyridinium-based cationic surfactants, namely N-(n-octyl)-2-methylpyridinium bromide (MP8),N-(n-decyl)-2-methylpyridinium bromide (MP10), and N-(n-dodecyl)-2-methylpyridinium bromide (MP12). The synthesized surfactants were characterized by Fourier Transform Infrared (FT-IR) and Nuclear Magnetic Resonance (NMR) spectroscopy, and their critical micelle concentration values were determined using the conductivity measurement technique. Weight-loss measurements, Potentiodynamic polarization, Electrochemical Impedance Spectroscopy (EIS), Scanning Electron Microscope with Energy Dispersive X-ray Spectroscopy (SEM/EDX) and Density Functional Theory (DFT) calculations were used for the assessment of corrosion inhibition performance. The lower CMC was correlated with an increase in the length of the alkyl chains (MP8<MP10<MP12), and the inhibition efficiency also increased. Weight-loss tests showed that MP12 (90%), MP10 (89%) and MP8 (88%) gave better results for adsorption on the surface of steel for which a compact protective film was formed, and electrochemical tests (MP8 < MP10 < MP12) showed increasing the alkyl chain ;length from MP8 to MP12 increased the hydrophobic character of the surfactants, which promoted molecular aggregation at lower concentrations, decreased the CMC, enhanced adsorption and protective film formation on the steel surface, and consequently improved the corrosion inhibition performance and adsorption tests showed the same trend. The potentiodynamic polarization i_{corr} ($\mu A/cm^2$) results showed that the prepared surfactants inhibited in mixed type while by EIS measurements the charge transfer resistance R_{ct} increased and double layer capacitance (C_{dl}) values were decreased as the inhibitor concentration increased. Surface deterioration results were confirmed by SEM/EDX test which showed less surface deterioration where the inhibitors were present. The adsorption sites were determined through (DFT) calculations assisted with the help of the Mulliken population analysis and Fukui indices and it was found that as the alkyl chain length increased the adsorption strength and corrosion inhibition was increased. The combined experimental and theoretical results obtained indicated that the critical micelle concentration (CMC) played a vital role in the mechanism of adsorption and corrosion inhibition and could help in the rational design of the surfactant-based corrosion inhibitors.

Keywords: Corrosion Inhibition, Surfactants, Mild Steel, Electrochemistry, Fukui Indices

1. Introduction

Corrosion is a natural phenomenon that occurs when the metals deteriorate gradually as a consequence of the influence of the surrounding environment like moisture, media of corrosion and oxygen that leads to structural damage, mechanical failure and huge economic losses [1]. Due to its good mechanical performance and low cost, mild steel is widely used in the petroleum, marine and automotive industries. It does, however, have a tendency to corrosion in chloride rich acidic environment which restricts its use in industries. Higher acidity levels help with Fe dissolution with the formation of soluble Fe^{2+} ions, and chloride ions help to penetrate the oxide and promote localized corrosion. The

simultaneous action of an acidic environment and chloride ions causes a greater rate of dissolution of the metal and degradation of the surface [2].

Cationic surfactants have become an interesting group of compounds as corrosion inhibitors due to the simplicity of application, cost effectiveness and high inhibition efficiency [3]. Because of their amphiphilic structure they can adsorb on the metal surfaces and create a protective layer that blocks the metal's active corrosion sites. Corrosion protection is further increased by the presence of heteroatoms and π-electron systems in the organic compounds which are able to interact between the electron-rich centers and the unfilled d-orbitals of the metal atoms. Cationic surfactants, those containing the pyridinium group are especially interesting as surfactants because the pyridinium ring has heteroatoms and delocalized π-electrons which facilitate the adsorption by electrostatic attraction and donor-acceptor interaction. The hydrophobic alkyl chain also facilitates to form compact protecting film that makes pyridinium derivatives as promising corrosion inhibitor for mild steel [4]. The corrosion inhibitory effect of pyridines and quaternary ammonium compounds in acidic solutions has been well proved up to now. High inhibition efficiencies have been achieved for quaternary ammonium salts [1], pyridine derivatives [4], alkyl pyridine ionic liquids [5] , and di-cationic pyridinium [6] which were found to be influenced by alkyl chain length and structure of the molecular, respectively, and also for di-cationic pyridinium. However, the link between CMC, molecular adsorption, electrochemical behavior and quantum chemical descriptors is yet not well understood. Moreover, the effect of the combined influence of alkyl chain length on micellization, adsorption thermodynamics, surface morphology and electronic structure has not been investigated fully within a single experimental and theoretical context [7, 8].

In this work, a series of new pyridinium based cationic surfactant (MP8, MP10 and MP12) was synthesized and investigated as corrosion inhibitors for CR4 mild steel in a highly corrosive acidified chloride medium (3.5 wt.% NaCl at pH 1.5). This work aimed to synthesize a series of new pyridinium based organic cationic surfactants (MP8, MP10 and MP12) and evaluate their performance as corrosion inhibitor in highly corrosive acidified chloride medium (3.5 wt % NaCl and pH 1.5) to prevent corrosion of the CR4 mild steel. The study has systematically investigated the effect of the alkyl chain length on CMC, adsorption, electrochemical analysis, surface properties and theoretical property, while studying the corrosion inhibition mechanism under acidic–chloride environment by using the studied compounds.

2. Materials and methods

2.1. Materials, electrode

All chemicals and solvents were of analytical grade and used without further purification. 2-methylpyridine, 1-bromooctane, 1-bromodecane, 1-bromododecane, toluene, and diethyl ether (99%) were procured from Sigma-Aldrich (USA).

2.2. Electrolyte preparation

A CR4 mild steel working electrode (0.07 cm²) was prepared with chemical composition as described in table S1 and polished to a mirror-like finish before each experiment. An aqueous 3.5 wt.% NaCl solution adjusted to pH 1.5 with 0.1 M HCl was used as the blank electrolyte. The synthesized surfactants were added to obtain concentrations of 0.5–15.0 mM, and the solution pH (1.50 ± 0.01) was maintained throughout the experiments. The selected acidified NaCl medium represents a highly aggressive chloride environment and is widely used to evaluate adsorption-based corrosion inhibition under severe corrosion conditions.

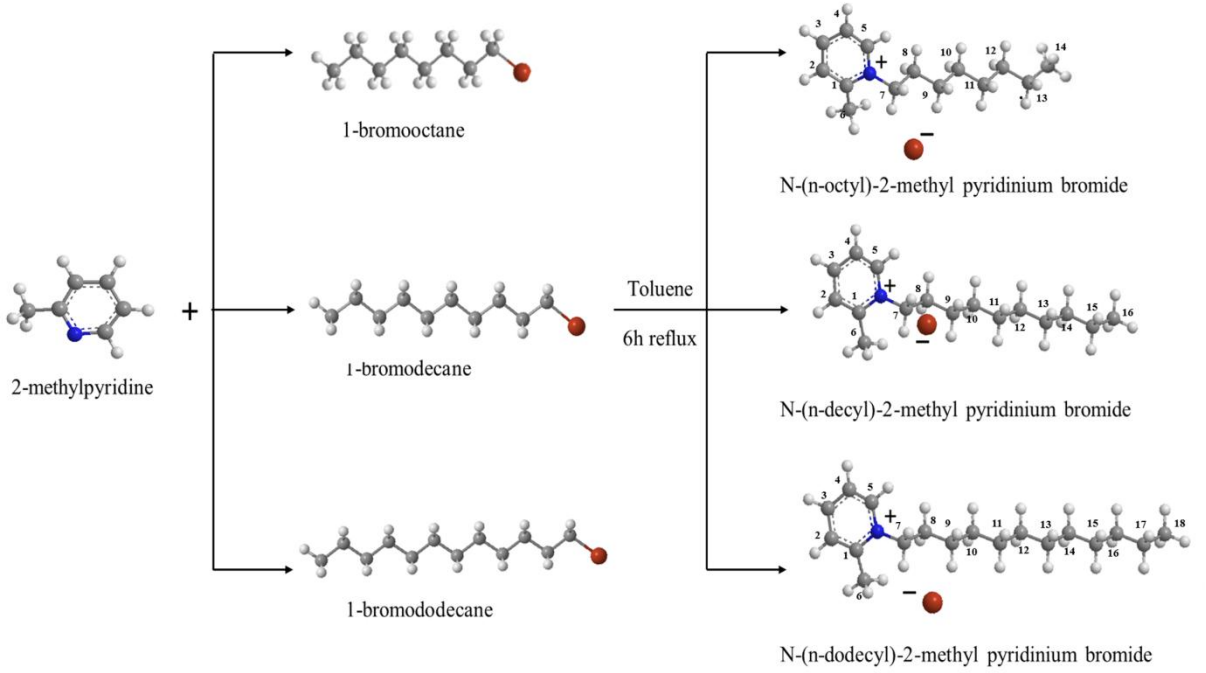

Figure 1. Synthetic pathway of surfactants MPn (n= 8,10 and 12).

2.3. Synthesis of inhibitors

Pyridinium-based surfactants were prepared by reacting 2-methylpyridine with the respective 1-bromoalkanes (C8, C10 and C12) in 1:1 molar ratio. Reactions were all performed in anhydrous toluene, under reflux (103–104 °C) for 12 h. These MP8 and MP10 were liquid–liquid separated, washed with diethyl ether for purity, while MP12 was obtained as a solid precipitate which was later filtered, washed with diethyl ether for purity and dried in vacuo before characterization. The synthetic route is presented in figure 1; FT-IR, ^{1}H NMR and ^{13}C NMR characterization data are presented in the Supplementary Information.

2.4. Critical micelle concentration (CMC)

Conductivity measurements were made at 298 K using different concentrations of the surfactant solutions to calculate the critical micelle concentration (CMC) of the synthesized surfactants. The CMC was determined from the conductivity–concentration plot, where the conductivity curve changes slope, corresponding to the CMC. All measurements were done three times and the reported values are the average of three different measurements.

2.5. Weight loss method

Mild steel coupons (1.105cm²) were prepared as mentioned in Section 2.1 and dipped in the corrosive solution containing varying concentrations of the inhibitor for 24 hours at ambient conditions. The coupons were removed from the immersion, cleaned, dried and then reweighed. Each test was carried out three times and the corrosion rate, inhibition efficiency and surface coverage was calculated from the weight-loss measurements.

Also, the adsorption behavior of the synthesized surfactants on the CR4 mild-steel surface was evaluated using adsorption isotherm analysis. The surface coverage (θ) obtained at different inhibitor concentrations was fitted to the Langmuir adsorption isotherm by plotting C/θ against C according to Equation (1). The adsorption equilibrium constant (K_{ads}) was determined from the Langmuir plot. The standard Gibbs free energy of adsorption ($\Delta G°_{ads}$) was subsequently calculated from K_{ads} using Equation (2).

$$\frac{C}{\theta} = \frac{1}{Kads} + C \qquad (1)$$

$$-\Delta G^{o}_{ads} = RT \ln (55.5\ K_{ads}) \quad (2)$$

where R is the universal gas constant, T is the absolute temperature, K_{ads} is the adsorption equilibrium constant, and 55.5 represents the molar concentration of water.

2.6. Electrochemical measurements

The electrochemical behavior of the CR4 mild steel in 3.5 wt.% NaCl solution (pH 1.5) has been examined in a traditional three-electrode cell (Gamry interface 1010e) using potentiostat/galvanostat. Potentiodynamic polarization (PDP) was measured after 3000 s of stabilization from −250 mV to +250 mV from OCP at a scan rate of 0.2 mVs^{-1} and electrochemical impedance spectroscopy (EIS) was performed over a frequency range of 100 mHz to 100 kHz using a ±5mV AC applied perturbation. All experiments took a triple repetition.

2.7. Surface Analysis (SEM/EDX)

The surface morphology of the CR4 mild steel after being immersed for 6 h in 3.5 wt. % NaCl with pH 1.5 (without and without inhibitors) was studied by scanning electron microscopy (SEM). To analyze the composition of the steel surface after treatment in blank solution, 10 mM of MP8, MP10 and MP12 surfactant solutions, energy-dispersive X-ray (EDX) spectroscopy was performed.

2.8. Quantum chemical calculations

Calculations using Gaussian 09 were carried out at the 6-311G level of theory using density functional theory (DFT/B3LYP). The molecules synthesized were subjected to geometrical optimization, determination of the vibrational frequencies, and their electronic properties. Importantly, there were no imaginary (negative) frequencies, and this was an indication that the optimized structures were true minima. On the basis of the optimized geometries, quantum chemical parameters that are pertinent to the corrosion inhibition, namely E_{HOMO}, E_{LUMO}, IP (I), EA (A), electronegativity (χ), hardness (η) and electron transfer (ΔN) were computed. The values of E_{HOMO} and E_{LUMO} values were used to calculate the ionization potential and the electron affinity values by applying the Koopman's theory, meanwhile the value of ΔN was determined by the Pearson method.

$$\Delta N = \frac{\chi(Fe) + \chi(inh)}{2\left(\eta(Fe) + \eta(inh)\right)} = \frac{\varphi + \chi(inh)}{2\eta(inh)} \quad (3)$$

(Equation 3), where χ_{Fe} = 7 eV and η_{Fe} = 0. Fukui indices for all the cationic, anionic and neutral molecules of the three inhibitors have been also calculated by natural bond orbital analysis [9].

3. Results and discussion

3.1. Characterization of synthesized surfactants

The synthesized surfactants were characterized, using ^{1}H NMR, ^{13}C NMR and FT-IR spectroscopy. The atom numbering for the assignment of the spectra is displayed in figure 1, and full spectroscopic data are available in the Supporting Information. In case of MP8, MP10 and MP12, bands in their FT-IR spectra at 1300 and 1307 cm^{-1} showed the attachment of the alkyl chain to the pyridine N atom. This was corroborated by the presence of H7 and C7 signal at around 4.7 ppm and 58.4 ppm in ^{1}H NMR spectrum and ^{13}C NMR spectrum respectively. The structure modification was verified by a downfield shift of the H7 by 3.4 ppm and of the C7 by 33.7 ppm when compared to the starting alkyl bromides. The assignments of the detailed spectra are included in the Supporting Information.

3.2. CMC measurements

At room temperature, the micellization behavior of the obtained surfactants were explored with conductivity measurements as a function of surfactant concentration (Figure 2). In the pre-micellar region, the rise on conductivity is faster because there is an increase in the concentration of the monomers and in the post-micellar region, the conductivity rise rate decelerated because the formation of micelle [10]. The overall conductivity continued to increase because of the migration of bromide ions between micelle surfaces, although at a slower rate. The (CMC) was determined from the intersection of the linear portions of the pre- and post-micellar regions [11]. The CMC values decreased with increasing alkyl chain length, reflecting the enhanced hydrophobic effect, as longer hydrophobic alkyl chains promote aggregation at lower concentrations to minimize contact with water molecules in figure 3 [12].

3.3. Weight loss measurements

Weight loss studies in the presence and absence of varying concentrations of MP8, MP10 and MP12 were conducted to determine the corrosion rate (k), inhibition efficiency (η%) and surface coverage (θ). The corrosion rate, inhibition efficiency and surface coverage were calculated using the following equations (4,5 and 6).

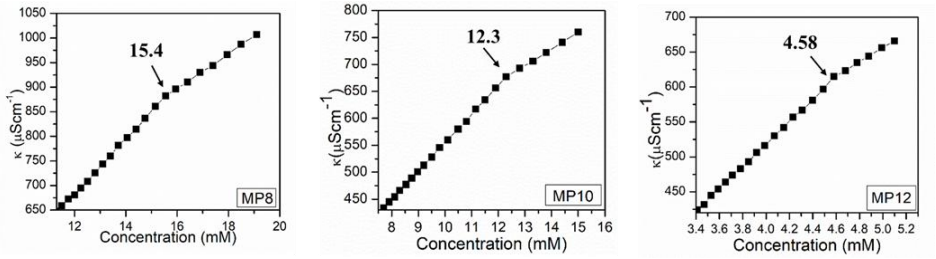

Figure 2. CMC curves of MP8, MP10, and MP12 at room temperature.

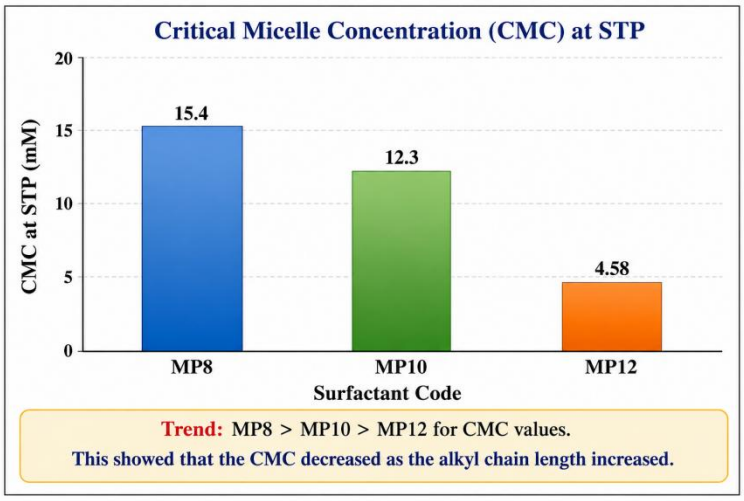

Figure 3. CMC of MP8, MP10, and MP12 in aqueous solution at STP.

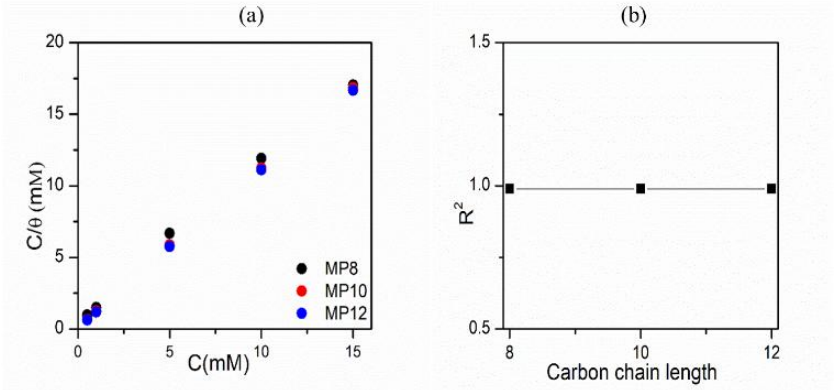

Figure 4. Langmuir adsorption isotherm for adsorption of synthesized inhibitors MP8, MP10, and MP12 over CR4 mild steel in corrosive media (a) Variation of the coefficient of determination (R^2) for MPn surfactants with carbon chain length (8, 10, and 12) (b).

Table 1. Weight loss parameters for CR4 mild steel in corrosive media containing different concentrations of inhibitors MP8, MP10, and MP12

	Concentration (mM)	Corrosion Rate k at 298 K ($mgcm^{-2}h^{-1}$)	Surface Coverage (θ)	Inhibition Efficiency %IE
BLANK		0.074532		
MP8	15	0.053982	0.88	88
	10	0.054078	0.84	70
	5	0.054166	0.75	69
	1	0.054215	0.67	67
	0.5	0.054322	0.52	52
MP10	15	0.037158	0.89	89
	10	0.040018	0.89	89
	5	0.040798	0.85	85
	1	0.041578	0.8	80
	0.5	0.042878	0.76	76
MP12	15	0.037679	0.9	90
	10	0.038978	0.9	90
	5	0.039495	0.9	90
	1	0.041319	0.85	85
	0.5	0.041836	0.82	82

Table 2. Adsorption parameters of MP8, MP10, and MP12 on the CR4 steel surface at 25°C in corrosive media.

	Concentration (mM)	C/θ (mM)	K_{ads}	R^2	Slope	$-\Delta G^{o}_{ads}$ ($kJmol^{-1}$)
MP8	15	17	15	0.99	1.11	16.6
	10	11.9	10			15.6
	5	6.7	5.1			14
	1	1.5	1.6			11.2
	0.5	0.9	1.5			11
MP10	15	16	15.1	0.99	1.11	16.6
	10	11.2	10			15.6
	5	5.8	5.2			14
	1	1.2	1.8			11.4
	0.5	0.6	2			11
MP12	15	16.8	15.1	0.99	1.11	16.7
	10	11.1	10.1			15.6
	5	5.7	5.2			14
	1	1.2	1.8			11.4
	0.5	0.6	2.1			11.1

From gravimetric results (Table 1), it was observed that the inhibition efficiency increased and the corrosion rate decreased with the increase in the surfactant concentration that also gave the maximum value in surface coverage. The inhibition efficiency of the three was found to be in the order, MP12 > MP10 > MP8, suggesting the critical role of alkyl chain length in inhibiting the corrosion activity. The longer the surfactant alkyl chain the more compact and stable the adsorbed monolayer and hence the higher was the inhibition efficiency [13]. Based on this, the corrosion rate decreased with an increase in inhibitor concentrations since the binding and attachment of the surfactant molecules to the surface increased with increasing concentrations, and this reduced the probability of the corrosive species being able to reach the steel surface

$$k = \frac{\Delta W}{s \times t} \qquad (4)$$

$$\eta\% = \left[\frac{W^{o} - W^{i}}{W^{o}}\right] \times 100 \qquad (5)$$

$$\theta = \frac{W^{o} - W^{i}}{W^{o}} \qquad (6)$$

3.3.1. Adsorption isotherm

The calculated adsorption parameters ΔG°_{ads}, K_{ads} and slope and R^2 are summarized in table 2 while the Langmuir plots for MP8, MP10, and MP12 are shown in figure 4. The slope was

close to 1 which showed that the adsorption of the synthesis of surfactant followed the Langmuir adsorption isotherm, suggesting the formation of predominantly monolayer adsorbed film [14]. This model assumes that adsorption and desorption are in equilibrium at a given time, that the binding site energies are equal, that one adsorbate molecule is bound to one binding site and that there are no significant lateral interactions. Alternative adsorption models did not result in a significant improvement in the quality of the fit or in the physical interpretation. For this reason, the Langmuir model fits very well (R^2 near 1) and was deemed adequate to describe the adsorption behavior of the synthesized surfactants [15].

The $\Delta G°_{ads}$ values are negative showing the adsorption process is spontaneous thermodynamically [16]. The magnitudes of ΔG°ads were below approximately -20 kJ mol^{-1}, which is generally consistent with predominantly physical adsorption [17, 18]. The investigated surfactants showed that MP12 had the most negative ΔG°ads value (−16.7 kJ mol^{-1}) which is comparatively high which shows that the surfactant is well adsorbed on the surface of the mild-steel. This was in agreement with the gravimetric results, where MP12 exhibited the maximum inhibition efficiency. The increased adsorption of MP12 therefore may relate to its longer hydrophobic alkyl chain, as well as to better surface coverage [1].

It is also known from the previous studies with pyridinium-based corrosion inhibitors that the relationship between the adsorption strength and the inhibition performance is also close. For instance, pyridinium type of cationic surfactant has been reported to adsorb spontaneously on mild steel, the relative proportion of physical and chemical adsorption being dependent on the molecular structure and $\Delta G°_{ads}$ [5].

3.4. Open circuit potential

In order to evaluate the electrochemical stability of the CR4 mild steel/electrolyte interface, the open-circuit potential (OCP) was measured under zero current conditions. Each electrochemical measurement was preceded by an OCP measurement until a steady potential was reached and the equilibration time was taken as 300 s, which is assumed to be quite long to reach a pseudo-steady state.

The OCP–time data for the CR4 mild steel in the absence and presence of the synthesized surfactants in a 3.5 wt.% NaCl solution (pH 1.5) are shown in figure 5. The OCP remained at around −0.52 V in respect to Ag/AgCl in the uninhibited solution while 15 mM MP8, MP10 and MP12 were able to move the OCP to −0.46, −0.48 and −0.49 V respectively. These small positive changes are believed to be due to electrochemical phenomena occurring at the interface of the metal/electrolyte and slight changes in the film of adsorption [19]. This is consistent with the trend of the inhibition found by the gravimetric data however the slight potential shifts alone do not give quantitative evidence of the corrosion inhibition.

3.5. Potentiodynamic polarization

The cathodic and anodic electrochemical reactions at the mildly corroded surface of the CR4 mild steel were investigated at the CR4 mild steel surface in the absence and presence of various concentrations of the synthesized surfactants at 25 °C as shown in figure 6. The anodic branch is the dissolution of iron to Fe^{2+} ions and the cathodic branch is the reduction of the H^+ ions to hydrogen gas. The electrochemical parameters such as corrosion potential (E_{corr}), cathodic Tafel slope (β_c), anodic Tafel slope (β_a), corrosion current density (i_{corr}) and inhibition efficiency (%IE) were computed for each inhibitor and is displayed in table 3. The corrosion current densities were extrapolated from the anodic and cathodic Tafel regions to corrosion potential to evaluate inhibition efficiency by using Eq. (7).

$$\%IE = \frac{i^{b}_{corr} - i^{i}_{corr}}{i^{b}_{corr}} \times 100 \quad (7)$$

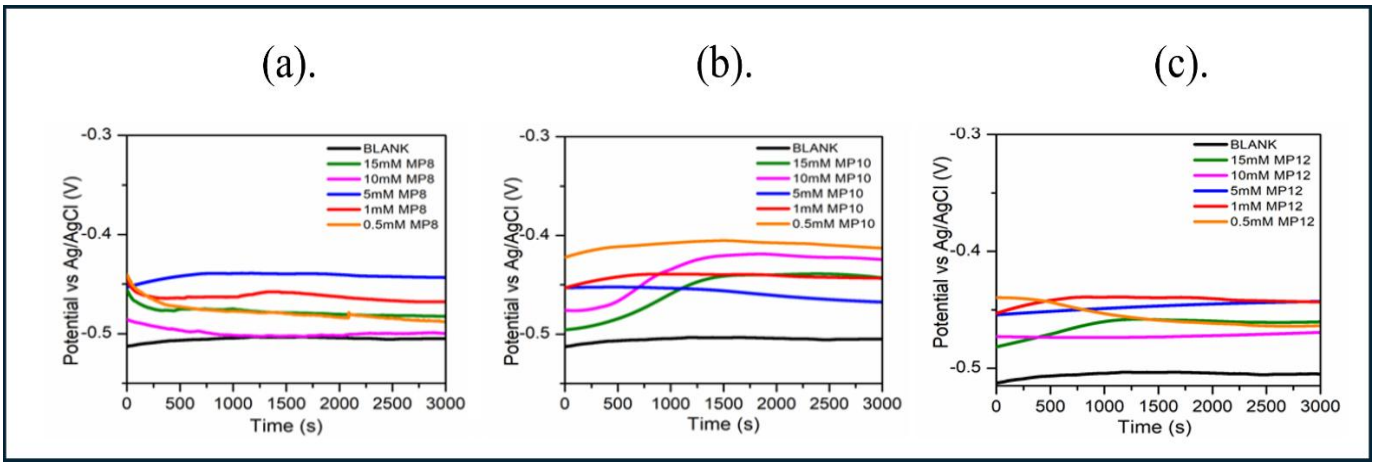

Figure 5. OCP vs. time curves of CR4 mild steel in corrosive media with and without different concentrations of inhibitors (a) MP8 (b) MP10 and (c) MP12.

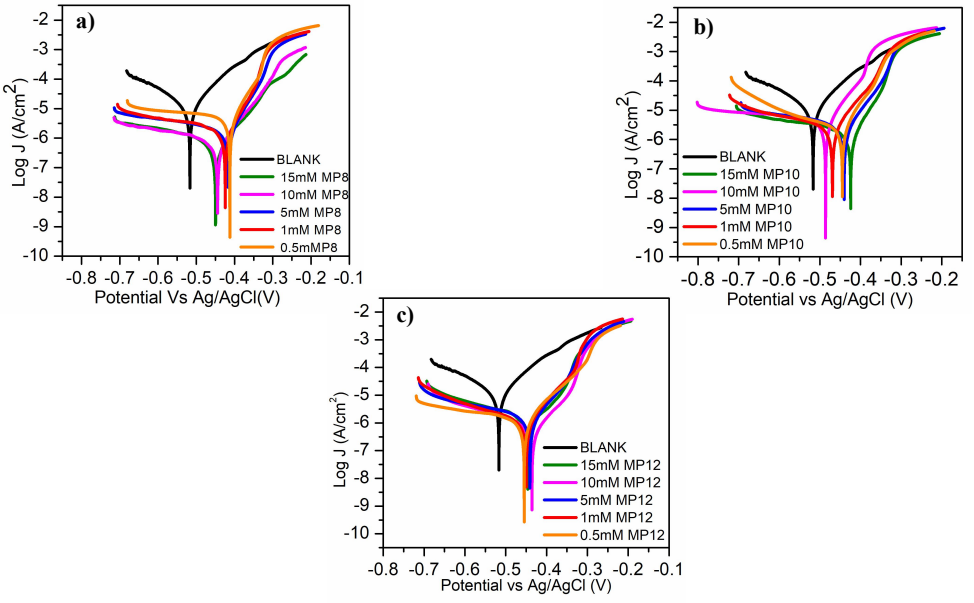

Figure 6. Polarization curves for CR4 mild steel in corrosive media with and without different concentrations of inhibitors (a) MP8 (b) MP10 and (c) MP12.

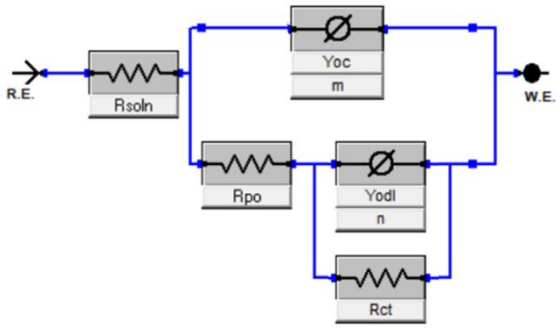

Figure 7. An equivalent circuit model applied for the corrosion studies of CR4 mild steel in corrosive media in the absence and presence of inhibitors.

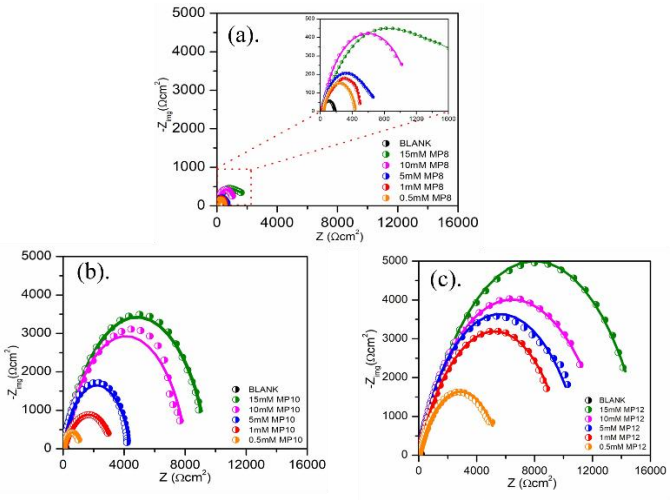

Figure 8. Nyquist plots for CR4 mild steel in corrosive media with and without different concentrations of inhibitors (a) MP8 (The inset presents a magnified view of the compressed semicircles at low impedance values) (b) MP10 (c) MP12.

Table 3. Potentiodynamic polarization parameters for CR4 mild steel with and without different concentrations of inhibitors in corrosive media.

	Concentration (mM)	β a (mV/Decade)	-βc (mV/Decade)	$-E_{corr}$ (Ag/AgCl) (mV)	i_{corr} (μA/cm^2)	IE (%)
BLANK		18.8	15.8	518	85.1	-
MP8	15	14.4	7.9	447	7.3	90
	10	15.9	2.6	449	23.8	72
	5	21.1	2.2	416	24.1	71
	1	21.4	2.7	438	25.2	70
	0.5	19.7	1.2	442	80.5	53
MP10	15	33.3	22.6	436	7.3	91
	10	19.6	8.6	484	7.6	91
	5	25.9	15.4	440	14.7	82
	1	23.5	12.9	470	16.5	80
	0.5	30.2	14.1	444	18	78
MP12	15	18.5	17	447	6.2	92
	10	20.4	14.4	434	6.5	92
	5	25.1	14.8	439	7.2	91
	1	20	9.8	449	9.1	89
	0.5	18.8	9.4	457	9.7	88

Table 4. EIS parameters for CR4 mild steel in corrosive media with and without different concentrations of inhibitors.

	Concentration (mM)	R_{po} (Ωcm^2)	R_{ct} (Ωcm^2)	Y_{odl} x10^{-6} (S x sa)	n	m	χ2 x 1	IE (%)
BLANK		26.74	156.5	1109	0.81	0.95	48.59	-
MP8	15	187.2	2036	72.3	0.25	0.66	285.7	92
	10	179.5	1734	337.2	0.63	0.76	348.8	90
	5	179.5	1734	14630	0.63	0.76	348.8	90
	1	22.6	1152	32.1	0.82	0.43	515.6	86
	0.5	40.07	396.8	194.6	0.83	0.76	68.4	60
MP10	15	3952	4087	19.3	1	0.78	894.2	96
	10	3968	4081	19.2	0.99	0.79	892.9	96
	5	476.2	4351	11.8	0.63	0.67	376.5	96
	1	7209	2226	17.5	1	0.79	326.5	92
	0.5	22.68	1153	32.4	0.82	0.44	515.7	86
MP12	15	3676	11920	8.142	0.48	0.77	252.1	98
	10	3755	9569	18.7	0.48	0.76	252.1	98
	5	4691	6815	20.3	0.47	0.77	275.8	97
	1	3676	6424	8.34	0.67	0.78	320	97
	0.5	246.4	5438	5.09	0.62	0.77	377.2	97

As seen in the absence of inhibitors (Figure 6), CR4 mild steel had a high corrosion current density, 85.1 μA cm^{-2} and an E_{corr} of −518 mV (Table 3). As per the gravimetric results the synthesized surfactants were all able to reduce the corrosion current density with the lowest seen at 15 mM of MP8, 7.3 μAcm^{-2}, MP10, 7.1 μAcm^{-2} and MP12, 8.5 μAcm^{-2}. The shift in the values of β_a and β_c reflects a mixed type of inhibition with adsorption on the metal surface [20, 21]. Only small positive changes of E_{corr} were observed, which should be seen in conjunction with the polarization and EIS results for interpretation of the corrosion behavior.

3.6. Electrochemical impedance spectroscopy (EIS)

Electrochemical impedance spectroscopy (EIS) was used to study the electrochemical behavior of the CR4 mild steel/electrolyte interface. The Nyquist plot, Bode plot and Bode phase plot were obtained at various inhibitor concentrations (Figures 8 and 9). The Nyquist plots showed one capacitive depressed loop and the Bode plots showed two phase-angle peaks that represent two time-constants for the corrosion process and the two processes taking place in the interface after the addition of the inhibitor. A fitting procedure was carried out with the experimental values obtained for the equivalent circuit model (Figure 7) to extract R_{soln}, R_{po}, Y_{odl} and R_{ct}. An ideal capacitor was replaced by a constant phase element (CPE) to consider the effect of the surface inhomogeneity, and the inhibition efficiency was calculated from R_{ct} by using Equation (9). Both the inhibited and uninhibited ones gave values of approaching unity, confirming essentially capacitively behaving

electrode/electrolyte interface.

$$Z_{CPE} = Y_o^{-1}(j\omega)^n \quad (8)$$

$$\%IE = \frac{R_{ct}^i - R_{ct}^b}{R_{ct}^i} \times 100 \quad (9)$$

Where R_{ct}^i and R_{ct}^b are the charge transfer resistance in the presence and absence of the inhibitor, respectively.

Nyquist plots for all the systems (Figure 8) had similar profile indicating that the corrosion mechanism remained unchanged with the presence of the prepared surfactants. However, the capacitive loop diameter was found to grow with inhibitor concentration and alkyl chain length meaning that charge-transfer resistance was higher, and that a more concentrated adsorbed layer was formed, thereby improving the corrosion inhibitor protection.

The Bode plots (Figure 9) corroborate the Nyquist plot. The magnitude of impedance (log Z) increased with the increase in alkyl chain length of each inhibitor in the whole range implying improvement in corrosion protection [22]. The phase angle also increased with the change to lower frequency suggesting the formation of a more protective and homogeneous interfacial film [23]. The results of these EIS studies show a good agreement with the gravimetric and polarization results and clearly show that the synthesized surfactants act as inhibitors and inhibit the corrosion process of CR4 mild steel by adsorption on the metal/electrolyte interface.

3.7. Surface analysis (SEM/EDX):

Figure 10 shows the SEM images of the surface of CR4 mild-steel before and after exposure to the corrosive medium in the absence and presence of MP12. MP12 was chosen as the representative inhibitor for surface characterization due to the best inhibition efficiency obtained in both gravimetric (Section 3.1) and electrochemical (Section 3.4 and 3.5) tests using the surfactants synthesized. Thus, the surface analysis is limited to the best inhibitor and offers morphological evidence for the inhibition trends found for the surfactant series [24] .

The polished surface of CR4 mild steel (Figure 10a) is relatively smooth, and is only mechanically treated with Emery paper during polishing. When exposed to the corrosive medium for 6 h without inhibitor (Figure 10b), the surface shows significant attack by the corrosive species which manifests itself as substantial roughness, irregularity and damage. Recently, similar transitions from a relatively smooth polished surface to a highly damaged and irregular surface morphology have been observed in uninhibited mild steel that is exposed to an acidic medium.

The CR4 specimen in the corrosive medium with 10 mM MP12 (Figure 10c) shows a much smoother surface with no visible damage in comparison to the uninhibited specimen. The substantial decrease in the surface deterioration is consistent with the adsorption of MP12 molecules at the steel/solution interface, creating a protective adsorbed layer which minimizes direct contact between the corrosive media and the metal surface. Similar SEM studies of pyridinium and surfactant corrosion inhibitors have been reported, and in those studies the surface of the inhibited steel contained significantly less surface damage than the uninhibited steel [7]. Recent reports [5] suggest that alkyl-pyridinium inhibitors could form a protective film on low-carbon steel and that the C12 alkyl-pyridinium one was more effective than the other short-chain inhibitors. This result is very similar to the present results in which the MP12 was found to have the highest inhibition efficiency in the series of surfactants investigated.

The better surface morphology observed in the presence of MP12 is also in agreement with the gravimetric and electrochemical results of the present study. The correlation between surface morphology and independent corrosion measurements confirms the proposed mechanism of protection by adsorption. This relatively high performance of MP12 could relate to the longer hydrophobic alkyl chain that may contribute to improved surface coverage and enhanced barrier between the metal surface and corrosive environment. The same has been reported for pyridine-based ionic-liquid inhibitors, in which the C12 derivative exhibited the best corrosion inhibition and surface protection effect. Therefore, SEM results give morphological evidence which complements the results obtained from the corrosion tests and shows that adsorption of MP12 significantly reduces corrosion induced surface deterioration of CR4 mild steel.

The EDX results in table 5 revealed that the steel surface after being polished had 95.7 wt.% Fe on its surface as seen in figure 11. In the blank solution (Figure 11h) the content of Fe was further reduced to 61.4 wt.% and the content of oxygen was increased to 32.8 wt.% which shows the formation of corrosion products. When MP12 was present (figure 11), the Fe content rose to 86.3 wt.% and the O content lowered to 3.8 wt.% which means the corrosion was drastically halted. A nitrogen peak (2.4 wt.%) was observed, but since it is close to the EDX detection limit, it was not considered as proof of inhibitor's adsorption. However, the alteration of the Fe and O contents is in line with the corrosion inhibition effect revealed by the gravimetric and electrochemical studies.

3.8. Theoretical studies

The inhibitors' ability to inhibit corrosion was examined using density functional theory (DFT). The optimized geometries (Figure 12) revealed that the molecules with the very long alkyl chains present twisted molecular structure. The C–Ar, C–N and aliphatic C–C bond lengths were ~ 1.50, 1.48 and 1.53 Å, respectively. The frontier molecular orbitals of the synthesized inhibitors are shown in figure 13. It was found that the HOMO was mostly located at the Br^- atom while the LUMO was mostly localized at the C and N atoms of the pyridinium ring. The frontier orbital energies (E_{HOMO} and E_{LUMO}) have been used to assess the corrosion inhibition potential. E_{HOMO} is the capability of inhibitor to donate its electrons for this formation of a protective layer on the metal surface and E_{LUMO} is the capability of inhibitor to accept electron and thus helping to the corrosion resistance.

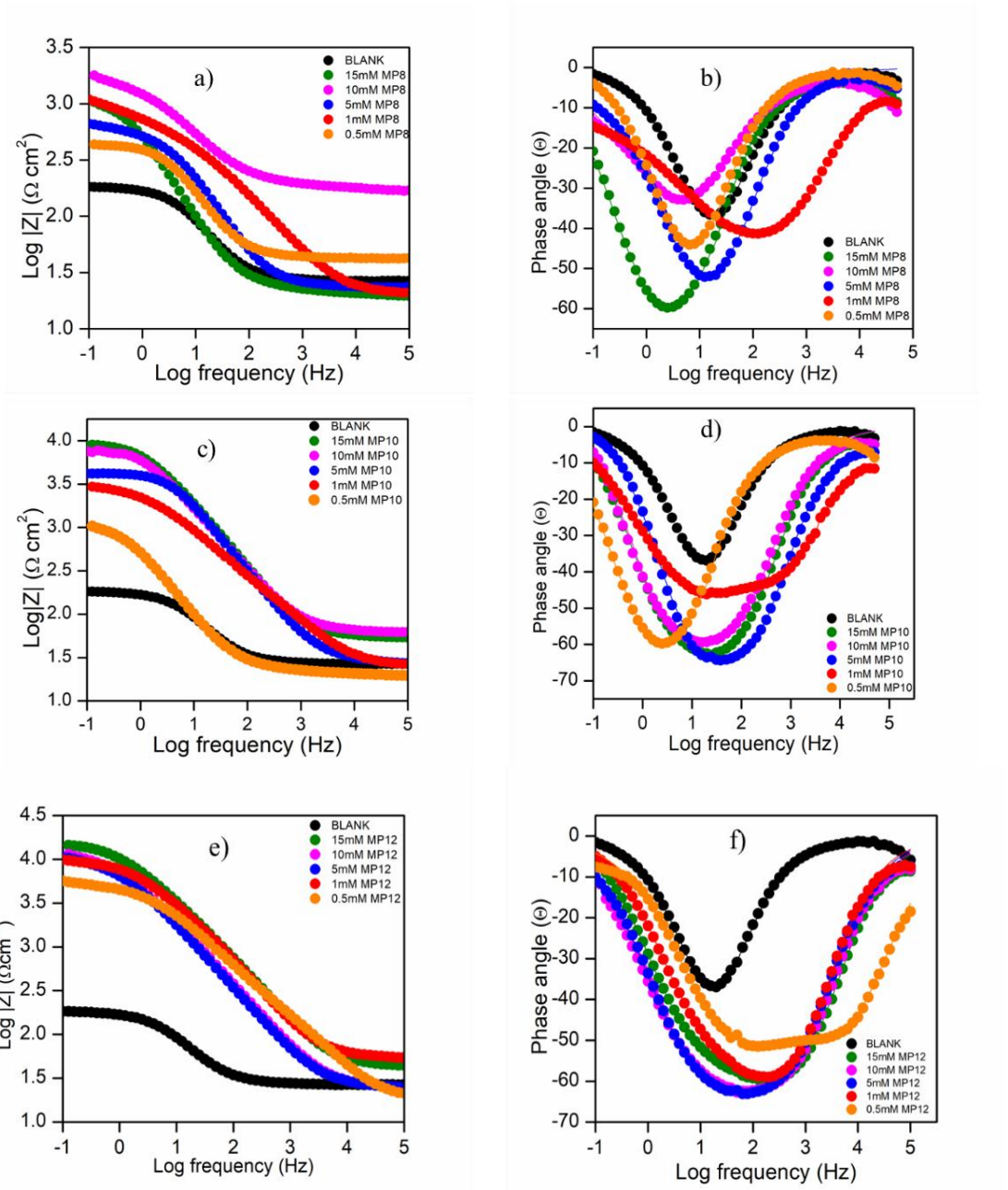

Figure 9. Bode plots for CR4 mild steel in corrosive media with and without different concentrations of inhibitors (a, b) MP8 (c, d) MP10 (e, f) MP12.

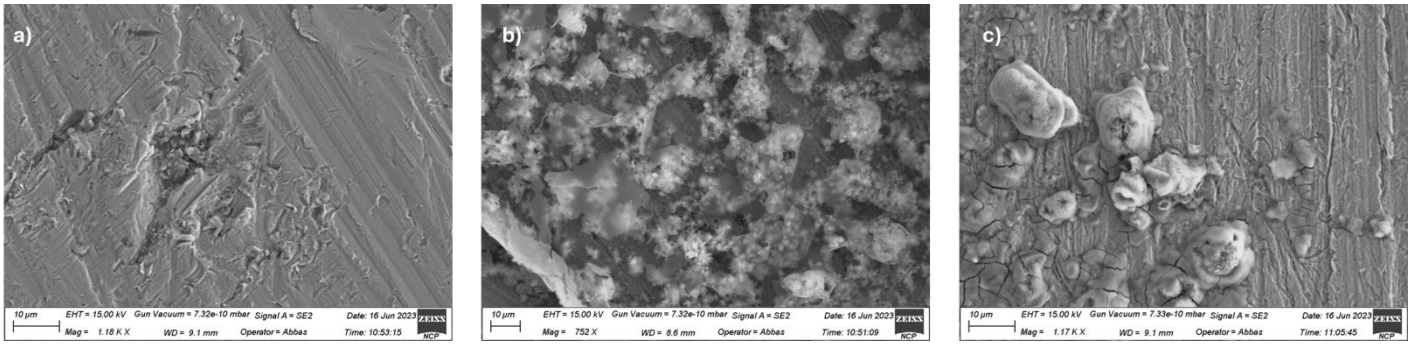

Figure 10. SEM images of CR4 mild steel (a) Polished (b) Immersed in 3.5% NaCl, at pH 1.5 without inhibitor (c) in the presence of 10 mM MP12.

Table 5. EDX data showing elemental percentages for Fe, C, O, Cl and N in the absence and presence of corrosion inhibitor MP12.

Element	Weight (%)		
Element	Polished Mild Steel	Mild Steel in Blank Solution	Mild Steel protected by MP12
Fe	95.7	61.4	86.3
C	4.3	5.6	7.5
O	-	32.8	3.8
Cl	-	0.2	-
N	-	-	2.4

Table 6. Quantum Chemical Parameters for synthesized inhibitors based on DFT/ B3LYP calculation in gas phase.

Inhibitors	EHOMO	ELUMO	ΔE	I	A	χ	H	ϭ	μ	ΔTC	ΔN
	(eV)	(eV)	(eV)	(eV)	(eV)	(eV)	(eV)	(e-1)	(D)		
MP8	-5.1901	-2.2251	2.996	5.1901	2.2251	-3.709	1.483	0.674	10.08	-0.37	3.61
MP10	-5.1883	-2.2256	2.9626	5.1883	2.2256	-3.707	1.481	0.675	10.11	-0.37	3.61
MP12	-5.1881	-2.2257	2.9624	5.1881	2.2257	-3.707	1.481	0.675	10.12	-0.37	3.61

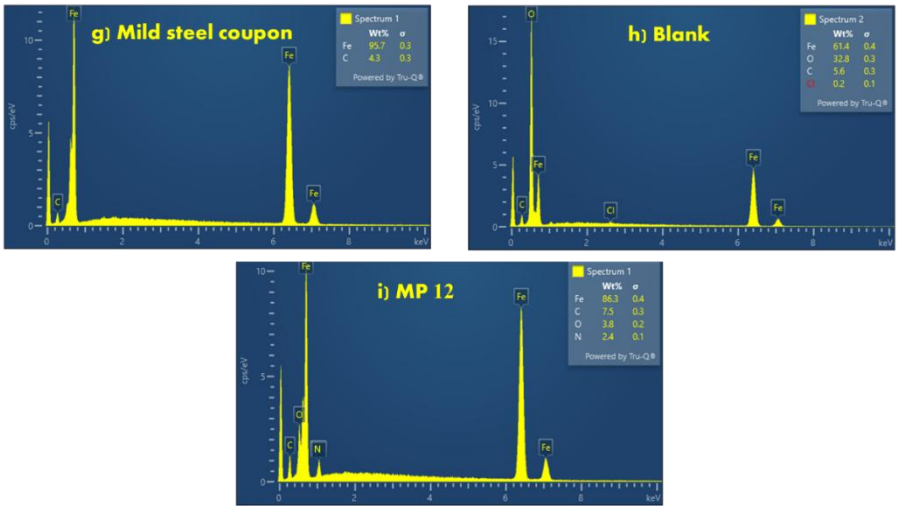

Figure 11. EDX images of CR4 mild steel (g) Polished (h) Immersed in 3.5% NaCl, at pH 1.5 without inhibitor (i) In the presence of MP12.

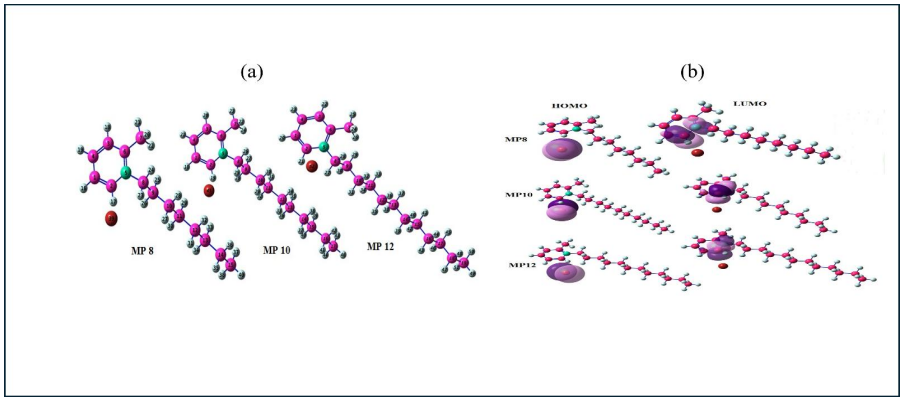

Figure 12. Optimized geometries of synthesized inhibitors (a & b).

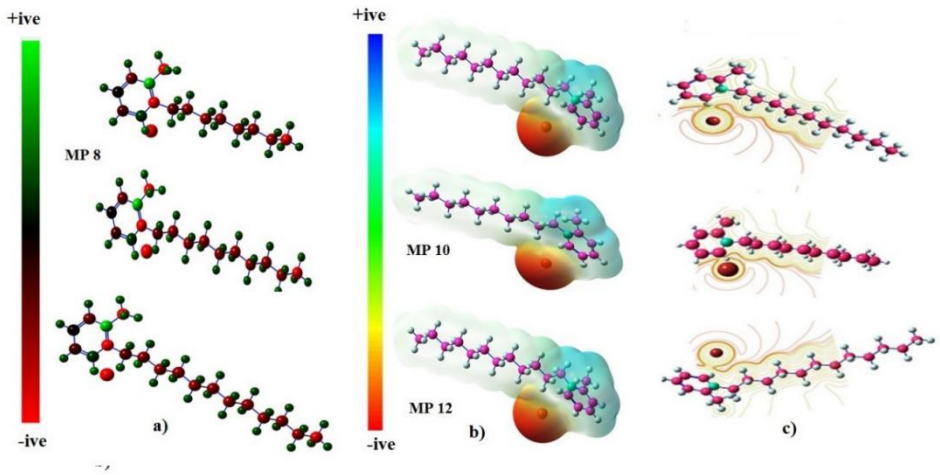

Figure 13. Visualization of a) Mullikan atomic charges b) Electron density mapping c) ESP distribution of synthesized inhibitors in gas phase.

Table 7. The Fukui functions on the C, N, Br atom of the studied inhibitor in the gas phase.

Atom	MP 8		MP 10		MP 12	
C1	-0.022	0.06	-0.022	-0.448	-0.021	0.0591
C2	-0.003	0.119	-0.003	0.119	-0.003	0.119
C3	0.038	0.009	-0.039	0.009	0.038	0.009
C4	0.059	0.163	0.058	163	0.055	0.163
N5	0.033	0.068	0.033	0.068	0.033	0.068
C6	0.048	0.093	0.049	0.093	0.053	0.093
C7	-0.016	-0.011	-0.016	-0.011	-0.016	-0.011
C8	-0.002	0.028	-0.002	0.027	-0.002	0.027
C9	0.017	-0.025	0.017	-0.025	0.017	-0.025
C10	-0.002	0.015	-0.002	0.016	-0.002	0.016
C11	-0.001	-0.002	0	-0.003	0	-0.003
C12	-0.001	-0.001	-0.001	0	-0.001	0
C13	0	-0.001	-0.001	-0.001	-0.001	-0.001
C14	-0.001	-0.001	0	0	0	-0.001
C15	0.001	0	0	-0.001	0	-0.001
C16	—	—	-0.001	-0.001	0	0
C17	—	—	—	0	0	-0.001
C18	—	—	—	—	-0.001	-0.001
C19	—	—	—	—	0	0
Br	0.672	0.248	0.536	0.246	0.546	0.346

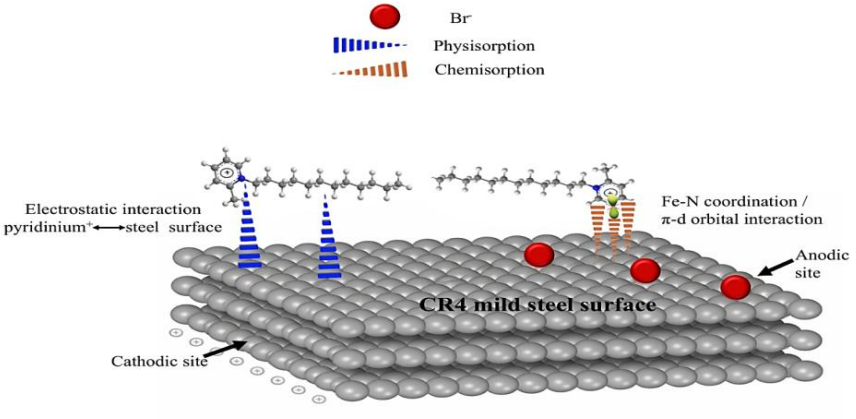

Figure 14. Adsorption mechanism of MPn (n=8, 10, 12) inhibitors over CR4 mild steel surface immersed in the corrosive media.

To assess the corrosion inhibiting activity of the synthesized surfactant, major electronic parameters such as band gap (ΔE) electronegativity (χ), softness (σ), hardness (η), electron transfer (ΔN) and total energy change (ΔTC) were considered as given in table 6. The E_{HOMO}, E_{LUMO} and ΔE values have been showing the order of inhibitive efficiencies for the said MP's as MP8 < MP10 < MP12. The more positive DMP and less electronegativity values of the synthesized inhibitors than the Fe show their tendency to donate electrons and improve adsorption. The softness and hardness values indicate that MP8 is a relatively less reactive material while the lower hardness value favors the corrosion inhibition. The negative ΔTC values (Equation 10) show that the electron back-donation from the Fe d-orbitals to the inhibitor molecules is feasible. The positive ΔN values confirmed that all the three inhibitors are capable of donating electrons to the metal surface [25], and the comparable values of ΔN and ΔTC parameters show that inhibition performance of the three surfactant compounds is not distinguishable by these parameters [26].

$$\Delta TC = -\frac{\eta}{4} \qquad (10)$$

The lack of any alteration in ΔN, χ, and ΔTC values of three inhibitors studied suggested that no alteration in the alkyl length was responsible for the alteration of electron donation and back donation potential. The adsorption sites of the inhibitor molecules in adsorption event on the metal surface were predicted using Mulliken population analysis. The former N atom (−0.627), the latter terminal C atom (−0.513) of the alkyl chain, and the C atom (−0.635) of the substituent methyl group were found to be the most negatively charged atoms and these were determined as the preferred adsorption sites due to the donor–acceptor interactions. The terminal carbon atom has better adsorption which enables improved adsorption and the longer alkyl chain of MP12 has better corrosion inhibition. The adsorption sites were also corroborated by the electrostatic potential maps (Figure 14) revealing an electron rich area around the Br atom and the electron poor area surrounding the pyridinium ring containing the N atom.

The Fukui index for electrophilic and nucleophilic attack were computed using Eqs. (11) and (12). The calculated Fukui indices of MP8, MP10 and MP12 are listed in the table 7. Highest values of f_k^- were found for the high reactivity positions of C2, C4 of the aromatic ring and were 0.119 and 0.163 respectively. It was observed that the f_k^+ values of Br-atom are higher than the f_k^- values as it is found to be a more susceptible electrophilic attack.

$$f_k^+ = q_k(N+1) - q_k \qquad (11)$$

$$f_k^- = q_k - q_k\,(N-1) \qquad (12)$$

3.9 Proposed Adsorption Mechanism and the Role of CMC in Corrosion Inhibition

The corrosion inhibitors studied in the present work are pyridinium based surfactants which are synthesized and the corrosion inhibition is realized by adsorption at the metal/electrolyte interface of CR4 mild steel [20, 27]. The gravimetric and electrochemical, adsorption and SEM/EDX and the theoretical results show that the process of inhibiting is both physisorption and chemisorption. The adsorption process is reinforced by a potential electrostatic effect between the potential pyridinium headgroup with its positive charge, and the evaluated surface of the metal, as well as by the interactions of π-electrons of pyridine ring with the empty d-orbitals of iron (Figure 14). That the HOMO, ΔN, ΔTC and Fukui indices have been calculated to support that interpretation.

The critical micelle concentration (CMC) plays an important role on the effectiveness of the synthesized surfactants. Surfactant molecules will adsorb on the surface of the mild steel below the CMC to create a compact protective monolayer which inhibits anodic iron dissolution and cathodic hydrogen evolution. The concentration at which the surface adsorption is essentially "saturated" is the same value as the CMC: above this concentration, additional molecules form micelles in the bulk solution, very few of which adsorb to the surface (Figure 15). In this case inhibition efficiency attains a saturation value and any further addition of inhibitor concentration does not show a significant change in inhibitor efficiency [28].

Surfactants with different alkyl chains show a strong influence on the adsorption behavior. The longer the hydrophobic alkyl groups, the more compact and stable will be the adsorption film and hence the more complete the surface coverage and the less aggressive chloride ion able to penetrate the film. This is because CMC of MP12 is lowest. Therefore, the corrosion inhibition efficiency of MP12 was highest, and MP10 and MP8 were next to it (Table 8). These results show that reducing the CMC facilitates efficient adsorption and hence good corrosion protection. From all of the above, it can be concluded that there is a correlation between molecular structure and surface activity, adsorption behavior and corrosion inhibition performance; thus, the proposed inhibition mechanism is direct.

A similar structure–activity relationship is seen in the present study. The corrosion-inhibition efficiency was the highest for MP12 followed by MP10 and MP8, while the lowest CMC was obtained for MP12 (Table 8). This is consistent with the increased hydrophobic properties of MP12, and its ability to form effective surface coverage. The overall results obtained from the experiments and theories show the correlation between molecular structure, surface activity, adsorption behavior and corrosion-inhibition performance of the synthesized pyridinium surfactants.

Table 8. Comparison of inhibition efficiency of synthesized surfactants.

Surfactants	CMC	Concentration	Weight Loss	Tafel Polarization	EIS
	(mM)	(mM)	%IE	%IE	%IE
MP8	15.4	20	88	90	92
		15	88	90	92
MP10	12.3	15	89	91	96
		10	89	91	96
MP12	4.58	10	88	92	98
		5	88	90	97

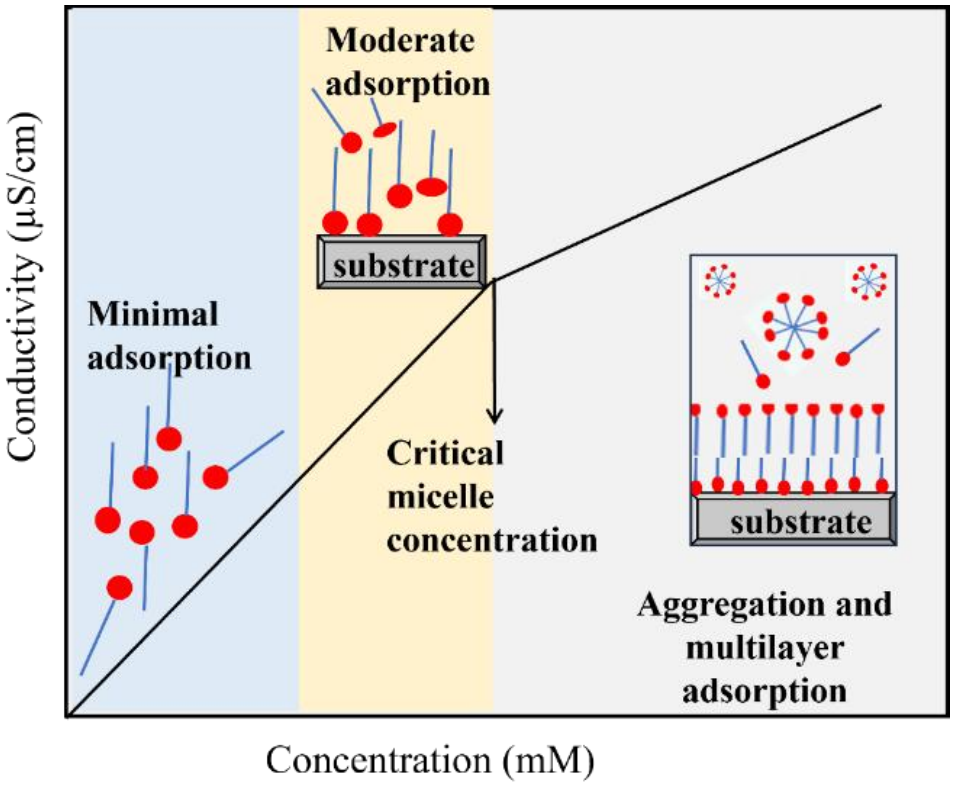

Figure 15. Effect of increasing concentration on surfactants adsorption.

4. Conclusion

In this study, MP8, MP10, and MP12 were successfully synthesized and characterized using FT-IR and NMR spectroscopy. Their critical micelle concentrations (CMCs) were determined using conductivity measurements. The synthesized surfactants were subsequently applied as corrosion inhibitors for CR4 mild steel in acidified chloride medium, and their inhibition performance was systematically evaluated using gravimetric and electrochemical techniques. The inhibition efficiency increased with increasing alkyl chain length in the order MP8 < MP10 < MP12. The adsorption of the surfactants on the mild-steel surface followed the Langmuir adsorption isotherm. The CMC played an important role in the inhibition process, as adsorption increased below the CMC, whereas further adsorption became limited after micelle formation. MP12 exhibited the highest inhibition efficiency because of its longer alkyl chain and lower CMC. Surface characterization and DFT calculations further supported the experimental observations. Overall, the gravimetric, electrochemical, adsorption, surface characterization, and theoretical results were consistent and confirmed the relationship between molecular structure, surface activity, adsorption behavior, and corrosion inhibition performance.

5. Future perspectives

The present study provides a comprehensive evaluation of pyridinium-based surfactants as corrosion inhibitors through gravimetric, electrochemical, surface characterization, and theoretical analyses. XPS and AFM would provide additional evidence regarding the protective layer. The influence of

temperature, micellization, environmental compatibility, and biodegradability should be investigated in future studies.

Author contributions

Maham Almas: Writing – original draft, Writing-review & editing, Conceptualization, Methodology, Investigation, Formal analysis, and Visualization. Rabia Talat: Writing-review & editing. Ubaid Ullah Khan: Conceptualization, Writing-original draft, Writing-review & editing, and Project administration. Ali Haider: Supervision, Investigation, and Writing-review & editing.

Ethical approval

Not applicable.

Conflicts of Interest

The authors report no conflicts of interest.

Acknowledgment

The authors are thankful to the Pakistan Academy of Sciences (PAS) for financial support through a research project funded in 2024. A.H. is also thankful to the Pakistan Science Foundation (PSF) for financial support through the research project PSF/Res/C-QAU/Chem(616).

Data availability statement

The data that support the findings of this study are available on request from the corresponding authors.

Supplementary material

The Supplementary Material for this article can be found online at:
https://www.jspae.com/index.php/jce/article/view/957/392

Funding

Not Applicable (N/A).

REFERENCES

1. Goni, L.K., et al., Synthesis of a new quaternary ammonium salt for efficient inhibition of mild steel corrosion in 15% HCl: Experimental and theoretical studies. Heliyon, 2024. 10(19).
2. SUHAILA, S., M.S.M. NOOR, and A. ARIFF, Three-dimensional model of ionic species concentration and flux during localised corrosion of steel in marine environment. JOURNAL OF ADVANCED RESEARCH, 2024. 25(1): p. 27-38.
3. Subramaniyam, S.S., et al., An overview of corrosion and its control by the surfactants: a mini-review. Canadian Metallurgical Quarterly, 2025. 64(4): p. 2182-2212.
4. Messaoudı, B., et al., Investigating the corrosion inhibition of copper using DFT theoretical study with three organic molecules. Turkish Computational and Theoretical Chemistry, 2024. 8(3): p. 54-65.
5. Luo, F., et al., Alkyl pyridine ionic liquid as a green corrosion inhibitor for mild steel in acidic medium. RSC advances, 2025. 15(33): p. 27369-27387.
6. Öztürk, S., et al., Resistance of di-cationic surfactant containing pyridinium ions to metal oxidation in 1.0 M HCl medium. Applied Surface Science, 2025. 692: p. 162741.
7. Yadav, C.K., et al., Effect of cetyl pyridinium chloride on corrosion inhibition of mild steel in acidic medium. International Journal of Electrochemical Science, 2024. 19(10): p. 100776.
8. Kuang, J., et al., PDINN as an Efficient and Environmentally Friendly Corrosion Inhibitor for Mild Steel in HCl: A Comprehensive Investigation. Coatings, 2025. 15(3): p. 352.
9. Marni, L.G., et al., Theoretical Study of Khellin Derivatives as Corrosion Inhibitors Based on Density Functional Theory (DFT). Turkish Computational and Theoretical Chemistry, 2024. 8(4): p. 36-47.
10. Jangde, D.T., et al., Solvent influence on the mixed micellization behavior of tailored ionic surfactants. Tenside Surfactants Detergents, 2026. 63(1): p. 1-15.
11. Silva, L.M. and J.J. Galan-Díaz, Comparative analysis of critical micelle concentration of cationic surfactants determined by conductivity, sound velocity, and density using weighted orthogonal distance regression. Surfaces and Interfaces, 2025. 56: p. 105620.
12. Yarahmadi, A., et al., Molecular design and thermodynamic insights into TnSm-type gemini surfactants for advanced interfacial applications. Scientific Reports, 2025. 15(1): p. 37097.
13. Jia, H., et al., Investigation of phosphorus-based ionic liquid with long alkyl chain as high-performance corrosion inhibitor with ultralow concentration for mild steel in 1 M HCl solution. Journal of Molecular Liquids, 2024. 396: p. 123946.
14. Kalam, S., et al., Surfactant adsorption isotherms: A review. ACS omega, 2021. 6(48): p. 32342.
15. Fan, J., et al., Investigations of synergistic effect of surfactants as corrosion inhibitor on steel. Surface Innovations, 2024. 12(3-4): p. 167-180.
16. Koufi, A., et al., Organic pyridinium salts as corrosion inhibitors for mild steel in acidic wastewater: experimental and DFT study. Coatings, 2026. 16(2): p. 148.
17. El-Maksoud, S.A.A., et al., Novel gemini cationic thiazole-based surfactants as carbon steel corrosion inhibitors in 1 M HCl using experimental and theoretical tools. Scientific Reports, 2025. 15(1): p. 17512.
18. Afaq, A., et al., Enhanced anticorrosion performance of antipyrine derivatives on mild steel in an acidic environment: an experimental and theoretical analysis. Materials Advances, 2026. 7(9): p. 4899-4927.
19. 19. Sawada, K., et al., Evaluation of corrosion potential stability of stainless steels in dilute electrolyte solution for application to a quasi-reference electrode used in electrochemical sensing system. Chemosensors, 2024. 13(1): p. 4.
20. Talat, R., et al., Evaluating the corrosion inhibition efficiency of pyridinium-based cationic surfactants for EN3B mild steel in acidic-chloride media. Coatings, 2022. 12(11): p. 1701.
21. Salim, R., et al., Inhibition behavior of new ecological corrosion inhibitors for mild steel, copper and aluminum in acidic environment: Theoretical and experimental investigation. Journal of Molecular Liquids, 2024. 393: p. 123579.
22. Hajjaji, F.E., et al., New imidazolium ionic liquids as ecofriendly corrosion inhibitors for mild steel in hydrochloric acid (1 M): Experimental and theoretical approach. Journal of the Taiwan Institute of Chemical Engineers, 2021. 123: p. 346-362.
23. Feng, L., et al., Synergistic corrosion inhibition effect of thiazolyl-based ionic liquids between anions and cations for

copper in HCl solution. Applied Surface Science, 2019. 483: p. 901-911.
24. Alharbi, M., et al., Insight into the time-dependent corrosion protection of mild steel by green ionic liquids: a combined electrochemical, surface, and computational study. RSC advances, 2025. 15(10): p. 8088-8101.
25. Zhang, Z., et al., Simultaneously enhancing mechanical and anti-corrosion properties of aluminum through electrodeposition of supersaturated Al (Fe) solid solutions. Applied Surface Science, 2024. 671: p. 160748.
26. Elabbasy, H., A. Toghan, and H. Gadow, Cysteine as an eco-friendly anticorrosion inhibitor for mild steel in various acidic solutions: electrochemical, adsorption, surface analysis, and quantum chemical calculations. ACS omega, 2024. 9(11): p.13391-13411.
27. Devi, Y.G., et al., Impacts of pyridinium gemini surfactants on corrosion inhibition of carbon steel. Surfaces and Interfaces, 2024. 45: p. 103796.
28. Ganjoo, R., et al., Coco monoethanolamide surfactant as a sustainable corrosion inhibitor for mild steel: theoretical and experimental investigations. Molecules, 2023. 28(4): p. 1581.

How to cite this article:
Almas, M., Talat, R., Khan, U. U., Fatima, S., Haider, A., Abbas, S. M., & Ali, S. (2026). Tailoring Hydrophobicity: Synthesis, Characterization and Application of Pyridinium-based Surfactants as Corrosion Inhibitors. Journal of Chemistry and Environment, 5(2). 1-16